# Absolute Momentum Calibration of the HARP TPC

**M.G. Catanesi, E. Radicioni**

*Università degli Studi e Sezione INFN, Bari, Italy*

**R. Edgecock, M. Ellis[1], F.J.P. Soler[2]**

*Rutherford Appleton Laboratory, Chilton, Didcot, UK*

**C. Gößling**

*Institut für Physik, Universität Dortmund, Germany*

**S. Bunyatov, A. Krasnoperov, B. Popov[3], V. Serdiouk, V. Tereschenko**

*Joint Institute for Nuclear Research, JINR Dubna, Russia*

**E. Di Capua, G. Vidal–Sitjes[4]**

*Università degli Studi e Sezione INFN, Ferrara, Italy*

**A. Artamonov[5], S. Giani, S. Gilardoni, P. Gorbunov[5], A. Grant, A. Grossheim[7], V. Ivanchenko[8], A. Kayis-Topaksu[9], J. Panman, I. Papadopoulos, E. Tcherniaev, I. Tsukerman[5], R. Veenhof, C. Wiebusch[10], P. Zucchelli[6,11]**

*CERN, Geneva, Switzerland*

**A. Blondel, S. Borghi[12], M.C. Morone[13], G. Prior[14], R. Schroeter**

*Section de Physique, Université de Genève, Switzerland*

**C. Meurer**

*Institut für Physik, Forschungszentrum Karlsruhe, Germany*

**U. Gastaldi**

*Laboratori Nazionali di Legnaro dell' INFN, Legnaro, Italy*

**G. B. Mills[15]**

*Los Alamos National Laboratory, Los Alamos, USA*

**J.S. Graulich[16], G. Grégoire**

*Institut de Physique Nucléaire, UCL, Louvain-la-Neuve,Belgium*

**M. Bonesini, F. Ferri**

*Sezione INFN Milano Bicocca, Università degli Studi Milano Bicocca, Milano, Italy*

**M. Kirsanov**

*Institute for Nuclear Research, Moscow, Russia*

**A. Bagulya, V. Grichine, N. Polukhina**

*P. N. Lebedev Institute of Physics (FIAN), Russian Academy of Sciences, Moscow, Russia*

**V. Palladino**

*Università "Federico II" e Sezione INFN, Napoli, Italy*

**L. Coney[15], D. Schmitz[15]**

*Columbia University, New York, USA*

**G. Barr, A. De Santo[17]**

*Nuclear and Astrophysics Laboratory, University of Oxford, UK*

**F. Bobisut, D. Gibin, A. Guglielmi, M. Mezzetto** [*]

*Università degli Studi e Sezione INFN, Padova, Italy*

**J. Dumarchez**

*LPNHE, Universités de Paris VI et VII, Paris, France*

**U. Dore**

*Università "La Sapienza" e Sezione INFN Roma I, Roma, Italy*

**D. Orestano, F. Pastore, A. Tonazzo, L. Tortora**

*Università degli Studi e Sezione INFN Roma III, Roma, Italy*

**C. Booth, L. Howlett**

*Dept. of Physics, University of Sheffield, UK*

**M. Bogomilov, M. Chizhov, D. Kolev, R. Tsenov**

*Faculty of Physics, St. Kliment Ohridski University, Sofia, Bulgaria*

**S. Piperov, P. Temnikov**

*Institute for Nuclear Research and Nuclear Energy, Academy of Sciences, Sofia, Bulgaria*

**M. Apollonio, P. Chimenti, G. Giannini**

*Università degli Studi e Sezione INFN, Trieste, Italy*

**J. Burguet–Castell, A. Cervera–Villanueva, J.J. Gómez–Cadenas, J. Martín–Albo, P. Novella, M. Sorel**

*Instituto de Física Corpuscular, IFIC, CSIC and Universidad de Valencia*

1

  *Now at FNAL, Batavia, Illinois, USA.*
[2]*Now at University of Glasgow, UK.*
[3]*Also supported by LPNHE, Paris, France.*
[4]*Now at Imperial College, University of London, UK.*
[5]*ITEP, Moscow, Russian Federation.*
[6]*Now at SpinX Technologies, Geneva, Switzerland.*
[7]*Now at TRIUMF, Vancouver, Canada*
[8]*On leave of absence from Ecoanalitica, Moscow State University, Moscow, Russia.*
[9]*Now at Çukurova University, Adana, Turkey.*
[10]*Now at III Phys. Inst. B, RWTH Aachen, Aachen, Germany.*
[11]*On leave of absence from INFN, Sezione di Ferrara, Italy.*
[12]*Now at CERN, Geneva, Switzerland.*
[13]*Now at Univerity of Rome Tor Vergata, Italy.*
[14]*Now at Lawrence Berkeley National Laboratory, Berkeley, California, USA.*
[15]*MiniBooNE Collaboration.*
[16]*Now at Section de Physique, Université de Genève, Switzerland, Switzerland.*
[17]*Now at Royal Holloway, University of London, UK.*

ABSTRACT: In the HARP experiment the large-angle spectrometer is using a cylindrical TPC as main tracking and particle identification detector. The momentum scale of reconstructed tracks in the TPC is the most important systematic error for the majority of kinematic bins used for the HARP measurements of the double-differential production cross-section of charged pions in proton interactions on nuclear targets at large angle. The HARP TPC operated with a number of hardware shortfalls and operational mistakes. Thus it was important to control and characterize its momentum calibration. While it was not possible to enter a direct particle beam into the sensitive volume of the TPC to calibrate the detector, a set of physical processes and detector properties were exploited to achieve a precise calibration of the apparatus. In the following we recall the main issues concerning the momentum measurement in the HARP TPC, and describe the cross-checks made to validate the momentum scale. As a conclusion, this analysis demonstrates that the measurement of momentum is correct within the published precision of 3%.

KEYWORDS: Time projection chambers, Detector alignment and calibration methods.

*Corresponding author, e-mail: Mauro.Mezzetto@pd.infn.it

# Contents

## 1. Introduction

The HARP experiment [1, 2] at the CERN PS was designed to make measurements of hadron yields from a large range of nuclear targets and for incident particle momenta from 1.5 GeV/$c$ to 15 GeV/$c$. The main aims are to measure pion yields for a quantitative design of the proton driver of a future neutrino factory, to provide hadron production cross-sections for precision calculations of the atmospheric neutrino flux [3] and to measure particle yields as input for the flux calculation of accelerator neutrino experiments, such as K2K [4], MiniBooNE and SciBooNE [5].
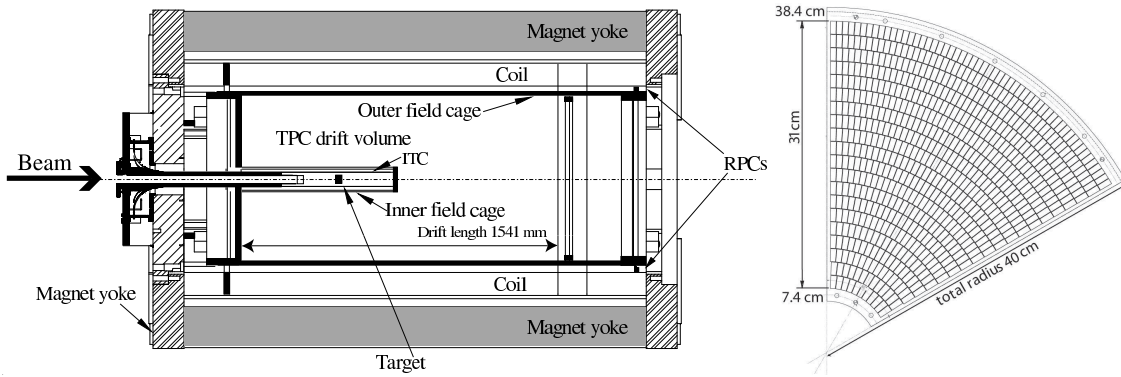
**Figure 1.** Left panel: schematic layout of the TPC. The beam enters from the left. Starting from the outside, first the return yoke of the magnet is seen, closed with an end-cap at the upstream end, and open at the downstream end. The field cage is positioned in the middle of the magnetic volume. The inner field cage is visible as a short cylinder entering from the left. The ITC trigger counter and target holder are located inside of the inner field cage. Right panel: mechanical drawing of a sector of the TPC pad plane, the layout of the pads is indicated.

The HARP experiment makes use of a large-acceptance spectrometer consisting of a forward and large-angle detection system. A detailed description of the experimental apparatus can be found in reference [2]. The forward spectrometer — based on large area drift chambers [6] and a dipole magnet complemented by a set of detectors for particle identification (PID): a time-of-flight wall [7] (TOFW), a large Cherenkov detector (CHE) and an electromagnetic calorimeter — covers polar angles up to 250 mrad which is well matched to the angular range of interest for the measurement of hadron production to calculate the properties of conventional neutrino beams.

The large-angle spectrometer — based on a Time Projection Chamber (TPC) and Resistive Plate Chambers (RPCs), located inside a solenoidal magnet — has a large acceptance in the momentum and angular range for the pions relevant to the production of the muons in a neutrino factory. It covers the large majority ($\sim$ 70%) of the pions accepted in the focusing system of a typical design.

## 1.1 The HARP TPC

The HARP TPC was designed and built in a record time of about 1.5 years. Its main design features are an almost full solid angle acceptance and high-event rate capabilities. It was operated in the years 2001 and 2002 at the CERN PS. Additional specialized calibration runs were performed in 2003.

The TPC consists of a cylindrical volume 1.5 m long and 0.8 m diameter filled with a 91% Ar, 9% $CH_4$ gas mixture positioned in a solenoidal magnet with a field of 0.7 T. A 12 kV electric field drives the ionization charges at a velocity of 5 cm/$\mu$s to the read-out plane, where the induction signals are collected by 3972 pads arranged in 20 concentric rows. The pad signals are digitized in 100 ns time bins, corresponding to about 5 mm bins in the longitudinal direction. A sketch of the HARP TPC and of its pad plane is shown in Fig. 1. More technical details can be found in reference [2]. The TPC is the key detector for the analysis of tracks emerging from the target at large angles with respect to the incoming beam direction.

The HARP TPC suffered from a number of shortcomings that were discovered during and after the data taking [2]:

1. A rather large number of deficient electronic channels ($\sim 15\%$) due to poor soldering of a fraction of cables to the back of the pad plane.

2. Static distortions caused by the inhomogeneity of the magnetic field, the accidental HV mismatch (about 2%) between the inner and outer field cage and edge effects near the inner and outer field cage.

3. Dynamic distortions caused by build up of ion-charge density in the drift volume during the 400 ms long beam spill, caused by a partial 'transparency' of the cathode wire grid. Given the beam intensity and the data acquisition rate with the 5% interaction length targets, it follows that HARP operated under conditions of a high dead time (higher than 90%). The number of events collected in each spill was on average about 300.

4. Cross-talk between pads caused by capacitive coupling between signal lines in the multilayer printed boards.

A description of the measures taken to correct for the effects of items 1, 2, and 4 is given in [2, 8]. The treatment of the dynamic distortions and some detail of the track fitting procedure are described in Appendix A. We recall here that in large angle cross section results published so far [8, 9], only the first part of the spill (about 30% of the total events), where the dynamic distortions are negligible were used (as discussed in Appendix A the distortions can be monitored by a physical parameter named $d'_\circ$). This provides very little penalty in measuring cross sections because already with this statistics systematic errors dominate in most of kinematic bins [8, 9].

Under these experimental conditions, in the absence of an appropriate calibration system and without the possibility of exposing the TPC to test-beams, a wide range of experimental cross-checks has been employed to assess the momentum scale in the HARP TPC, as described in the following.

## 1.2 Procedure used to determine the absolute calibration of the momentum scale

The momentum measurement in the HARP TPC is a direct result of the calculation based on the measured track curvature and the known magnetic field, no *ad hoc* correction factor has been applied to make the measurement agree with the benchmarks. Thus, the determination of the scale should be considered as a cross-check rather than a calibration.

A bias on the momentum scale as measured by a TPC is typically related to a sagitta error:

$$\delta(p_T)/p_T = s \cdot 8 \cdot q \cdot p_T/(0.3 \cdot B \cdot L^2) \tag{1.1}$$

Where the sagitta $s$ and the track length $L$ are in meters (0.5 m is the typical track length in HARP), the magnetic field $B$ in Tesla (0.7 T in HARP), the track momentum $p_T$ is in GeV/$c$, $q$ is the sign of the charge of the particle.

Unfortunately, it was not possible to send a direct beam of particles into the sensitive volume of the TPC. In the absence of such a beam, well defined procedures were used to determine the absolute calibration of the absolute momentum calibration of the TPC.

- The momentum scale in the TPC was characterized by using proton–proton elastic scattering data as benchmark, see Section 2, in two different ways:

  1. By using the incident proton momentum and direction (measured by the beam MWPCs) and the momentum and direction of the proton scattered at large angle, measured by the TPC, the missing mass squared $M_x^2$ is determined for every event (see Section 2.1). A bias in the momentum scale would reflect in a bias in the $M_x^2$ calculation.

  2. The angle of the forward scattered particle is used (measured by the forward spectrometer) together with the momentum and direction of the incoming proton to predict from the kinematics of the elastic scattering the recoil proton momentum and direction. This prediction is then compared with the measured momentum of the recoil proton (see Section 2.2). Special care has been devoted in this test to avoid any bias due to the different energy losses of protons (measured in elastic scattering events) against pions (cross section measurements), as described[1] in Section 2.2.3.

- As an additional cross-check, one can also look at the $dE/dx$ distribution, see Section 4. A satisfactory description of the $p$–$dE/dx$ distribution is obtained after the TPC calibration. Although less precise than the elastic scattering kinematics this method can be used to exclude large biases.

- A sagitta error would have opposite sign for positively and negatively charged particles and would grow linearly with $p_T$. It would thus be detectable, regardless of the absolute scale, by a dependence of the measured total momentum on the track angle for samples of tracks with different angles for which one can ensure that they have the same total momentum. These samples, as discussed in Section 4.2, can be defined using protons in fixed regions of relatively high $dE/dx$ ($dE/dx$ depends only on the total momentum).

- The $p$–$\beta$ relation using the time-of-flight measurement with the RPCs can also be used as a relatively weak cross-check, see Section 5. The precision of this method is limited by the understanding of the detector physics of the RPCs in combination with the very short flight-path.

## 2. Elastic scattering data

### 2.1 Measure of the missing mass squared

This analysis has been already published in [2] and it is only briefly summarized here. Events from the 3 GeV/$c$ momentum runs are selected by requiring standard beam selection criteria for protons and only 1 or 2 prong events in the TPC. The 2-prong events are determined by very loose kinematical cuts: $|(\phi_1 - \phi_2) - \pi| < 0.3$ rad and $(\theta_1 + \theta_2) < 1.75$ rad, where $\phi_1$, $\phi_2$, $\theta_1$, $\theta_2$ are, respectively, the azimuthal and polar angles of the two tracks. Further selection criteria are applied to the large-angle track, that is used for the final analysis: the particle is positively charged

---

[1]In principle it is enough to measure the angle of the scattered proton to predict its momentum. We did not follow this method because a) we use the angle to select a clean sample of elastic scattering events and b) the angle of protons is affected by multiple scattering in the material around the target
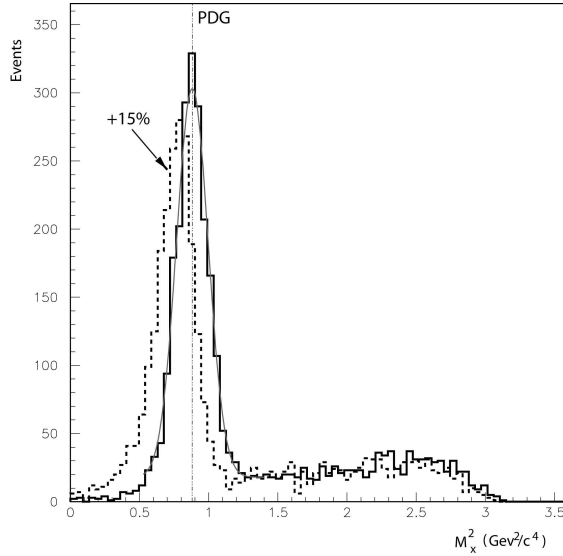
**Figure 2.** Missing mass in 3 GeV/$c$ pp scattering. The result (solid line) is centered very close to the PDG value of the squared proton mass. An artificial shift of 15% of the momentum measured was applied to obtain the dashed histogram. Such a shift is clearly excluded by the data (see the text).

and well measured over a minimum of 10 points; the reconstructed momentum is in the range $320 \, \mathrm{MeV}/c \leq p < 620 \, \mathrm{MeV}/c$. The tracks must come from the target[2] and must be recognized as a proton with a d$E$/d$x$ selection.

The missing mass is then computed as:

$$M_x^2 = (p_{\mathrm{beam}} + p_{\mathrm{target}} - p_{\mathrm{TPC}})^2 \tag{2.1}$$

where $p_{\mathrm{beam}}$, $p_{\mathrm{target}}$, $p_{\mathrm{TPC}}$ are the 4-momenta of the incoming beam particle, target particle and the particle scattered at large angle and measured in the TPC, respectively.

The result of this analysis is shown in Fig. 2. A fit to the distribution of Fig. 2 provides $\langle M_x^2 \rangle = 0.8819 \pm 0.0032 \, \mathrm{GeV}^2/c^4$ ($\chi^2$/ndof $= 20.5/17$ in the $0.55 - 1.4 \, \mathrm{GeV}^2/c^4$ range for a fit using a Gaussian plus a linear background as description) in agreement with the PDG value of $0.88035 \, \mathrm{GeV}^2/c^4$.

To study the effect of a momentum scale bias over the reconstructed missing mass, we have reconstructed the same distribution by displacing the momentum of the reconstructed track by 15%. As shown in Fig. 2 such a bias would produce a displacement of about $0.085 \, \mathrm{GeV}^2/c^4$ on $M_x^2$.

Systematic errors to this measurement come from uncertainties on the primary beam particle momentum, correction for proton energy losses in the material of the cryogenic target and inner field cage. As a result, the momentum scale is estimated to be correct to better than 3.5% (at one standard deviation).

---

[2]Longitudinal position of the point of minimum distance between the beam axis and the track extrapolation in the direction of the interaction vertex must be in the range of $-50 \, \mathrm{mm} \leq z < 70 \, \mathrm{mm}$, where $z$ is the coordinate along the beam direction

## 2.2 Comparison of the measured proton momentum with the elastic scattering predictions

Elastic scattering interactions of protons and pions off hydrogen provide events where the kinematics is fully determined by any of the kinematic quantities and in particular by the direction of the forward scattered beam particle. These kinematic properties of the elastic scattering reaction were exploited to provide a known 'beam' of protons pointing into the TPC sensitive volume. Data were taken with liquid hydrogen targets at beam momenta of 3 GeV/$c$, 5 GeV/$c$ and 8 GeV/$c$.

### 2.2.1 Data selection

A good fraction of forward scattered protons or pions in the elastic scattering reaction enter into the acceptance of the forward spectrometer (about 50% depending on the beam momentum).

Both direction and momentum of the recoil proton are then predicted.

Selecting events with one and only one track in the forward spectrometer and requiring that the measured momentum and angle of the forward track are consistent with an elastic reaction already provides an enriched sample of elastic events. To be counted, tracks need not to be inside the acceptance of the dipole magnet, but need only to be detected in the upstream drift chamber which covers the full acceptance of particles exiting the aperture of the solenoid magnet which houses the TPC. By requiring that only one barrel RPC hit is recorded at the position predicted for an elastic event (the precision of the prediction from the forward spectrometer is within the RPC pad size) and within a time window consistent with a proton time-of-flight, a sample of recoil protons with known momentum vector is obtained with a purity of about 99%.

The requirement of one RPC hit is relaxed for events where the recoil proton momentum is predicted to be low enough that it can be absorbed in the material in front of the RPCs. In such cases also events without any RPC hit are accepted. The additional requirement that the recoil angle is consistent with elastic scattering is then used to ensure a pure sample. At beam momenta in the range 3 GeV/$c$–8 GeV/$c$ the kinematics are such that these protons point into the TPC with angles of $\approx 70°$ with respect to the beam direction.

The correlation of the forward scattering angle and recoil proton momentum introduces an unavoidable threshold in recoil proton momentum ($\approx 350$ MeV/$c$) which translates into a minimum angle for the scattered particle. The threshold is relatively high due to the need to detect the proton also in the barrel RPC system outside the outer field cage of the TPC. As mentioned above, this requirement can be removed only in cases where a somewhat larger background can be tolerated.

Due to the geometry of the rectangular aperture of the dipole magnet of the forward spectrometer only two small horizontal sectors of the TPC can be populated with recoil protons above threshold momentum in the 3 GeV/$c$ beam. In the 5 GeV/$c$ beam the situation is much better and all azimuthal angles can be populated, although not yet homogeneously. In the 8 GeV/$c$ beam the population is homogeneous in $\phi$, but the error propagation of the measurement of the forward scattering angle into the prediction of momentum and angle of the recoil proton becomes less favorable.

The numbers of selected elastic events amount to about 15,000 for the 8 GeV/$c$ data sample, and 5,000 for each of the 5 GeV/$c$ and 3 GeV/$c$ data samples. The exposures with higher momentum beams have not been used for this study.
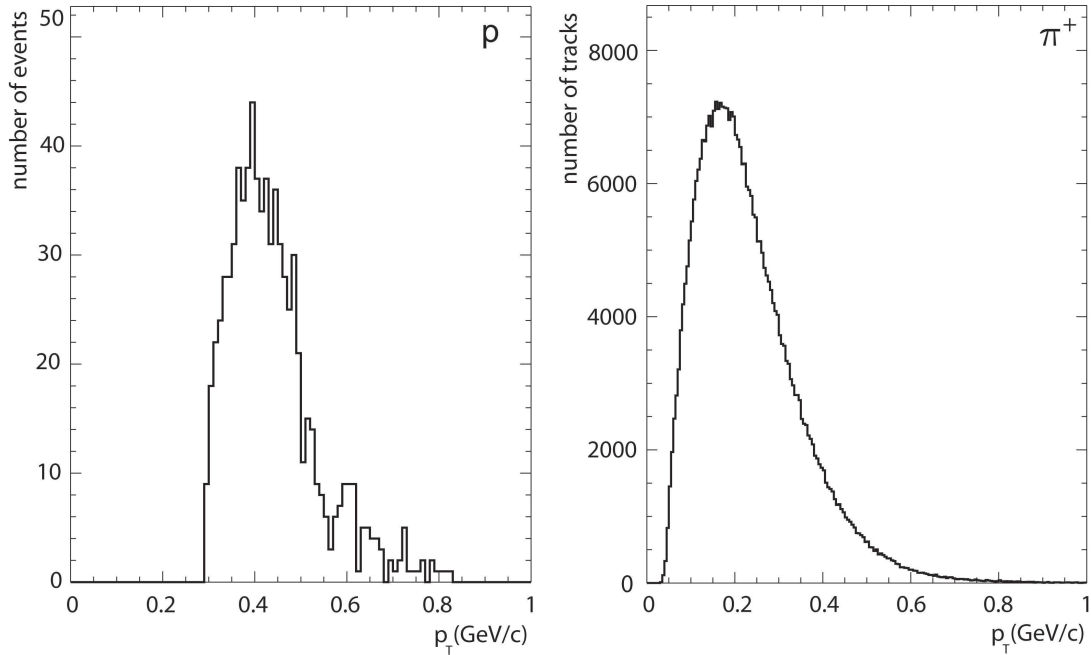
**Figure 3.** Left panel: $p_T$ of the recoil protons in used in the proton and pion elastic scattering data (5 GeV/$c$ runs) using the forward spectrometer to determine the kinematics. Right panel: typical distribution of the $p_T$ of pion tracks used in the cross section measurement for 8.9 GeV/$c$ p–Be interactions in the angular range of the analysis before $p$ and $p_T$ cuts.

### 2.2.2 Protons versus Pions

With elastic scattering we can check the reconstructed momentum of protons, while in cross section measurements we are interested in the momentum of pions. If the momentum scale is influenced by a bias, however, protons are a robust check provided that their momentum in elastic scattering events is similar to the momentum of pions in cross section measurements and that their higher energy losses do not influence the measurement. The comparison of the $p_T$ of protons from elastic events and the $p_T$ of pions in a typical setting, Fig. 3, shows that with elastic scattering most of the range of interest is covered.

The possibility that the energy loss of low momentum protons can alter the momentum reconstruction is discussed in the following section.

### 2.2.3 The "unconstrained fit"

Since the energy loss in the material of the cryogenic target, trigger counter, and inner field cage is large for protons in the energy range covered by elastic scattering, there is a significant change of curvature of their trajectory in that region of the detector. This effect introduces a bias in the measurement of the momentum if one uses the vertex constraint for these low-momentum protons. Therefore, the behaviour of the momentum measurement for protons was studied without making use of the vertex constraint. If one would use a vertex constraint in the fit for these protons one would either have to modify the algorithm to take into account the change of curvature induced by the large energy loss in the inner field cage or one would have to correct *a posteriori* for the bias.
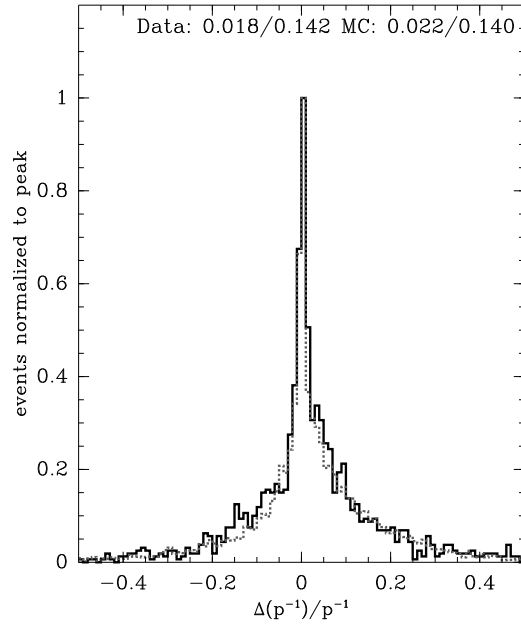
**Figure 4.** Comparison of the unconstrained ($p1$) and constrained ($p2$) momentum ($p1/p2 - 1$) for pions (above 350 MeV/$c$) using data (from different target materials) and the corresponding Monte Carlo. The data are indicated by the black histogram and the Monte Carlo by the dashed histogram. The position of the peak is at zero well within 1% and the mean is 2% both for data and MC. The first 50 events in the spill are used.

The former option, the use of a modified algorithm, would not validate the standard code used for the minimum ionizing pions. The latter option is used in the analysis described in Section 2.1. Inside the TPC gas volume the energy losses of protons are negligible so that they can indeed be used to validate the procedures in a way also applicable to the situation for pions.

Constrained and unconstrained fits are sensitive in the identical way to any sagitta error, since the vertex position is not influenced by distortions in the TPC.

For pions and high momentum protons it was checked independently that the constrained fit is unbiased with respect to the unconstrained fit for tracks reconstructed in the real data and in the simulated data. In Fig. 4 it is shown that the vertex constraint does not introduce biases for those particle trajectories and that the simulation provides an excellent description of the behaviour of the resolution function. The comparison of the unconstrained ($p1$) and constrained ($p2$) momentum ($p1/p2 - 1$) for data and Monte Carlo shows that the position of the peak is centered at zero well within 1% and that the average is about 2% both for data and MC.

### 2.2.4 Results with the standard data selection

In this comparison, only the first 50 events in the spill were used in order to avoid the effect of dynamic distortions in the unconstrained fit (see also Appendix A). Given the beam conditions of the run under study here, this condition guarantees the same data quality as in the analyses of references [8, 9].
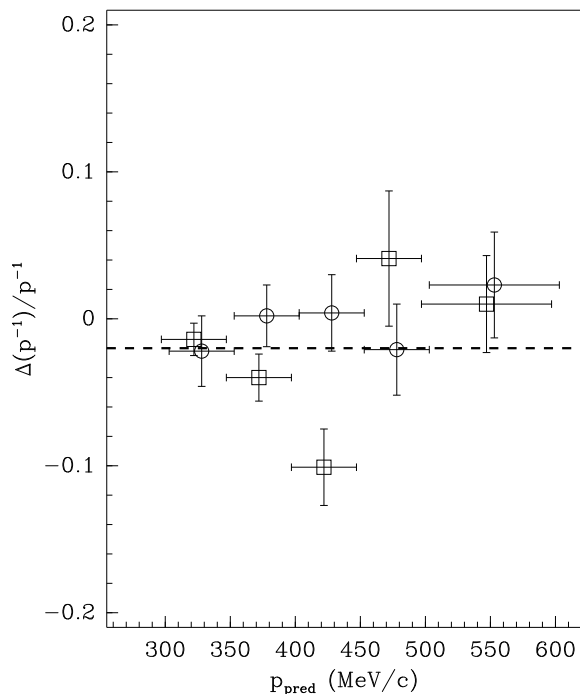
**Figure 5.** The momentum bias of the fit without vertex constraint measured with elastic scattering data (3 GeV/$c$: open squares, 5 GeV/$c$: open circles) as a function of the momentum predicted by the forward scattered track. In the absence of a clear trend, the average of the points constrains the bias to be smaller than 3%. For these comparisons only the first 50 events in the spill are used since the unconstrained fit is sensitive to dynamic distortions beyond this value.

The comparison of predicted momentum and the momentum reconstructed without vertex constraint is shown as a function of predicted momentum in Fig. 5. The relative average difference is $(2 \pm 1)$%, and shows no clear momentum dependence. From this observation one concludes that the momentum scale is known to better than 3% (at one standard deviation). Systematic uncertainties such as the absolute beam momentum scale, the precision in the measurement of the kinematic quantities of the forward scattered track and the need for energy loss corrections limit this test to a precision of about 2%. Since the sensitivity of the benchmark is similar to the shift observed it is not justified to adjust the momentum scale to the benchmark.

### 2.2.5 High statistics benchmarks

To improve the statistics of this check, we make use of the full statistics by applying the correction of the dynamic corrections (see Appendix A) and we add elastic scattering $\pi^+ - p$ events to the proton elastic scattering sample and analyse separately $\pi^- - p$ events [3]. One should note that the effect of a trajectory distortion creates the same momentum shift if a systematic shift on the sagitta is caused by an $E \times B$ effect, since both the effect and the curvature for protons change sign simultaneously. Therefore these two settings are expected to provide consistent results. The

---

[3]In the following figures the label "positives" indicates the recoil protons in elastic scattering events in the positive beam, and "negatives" is used to label the protons in the negative beam.
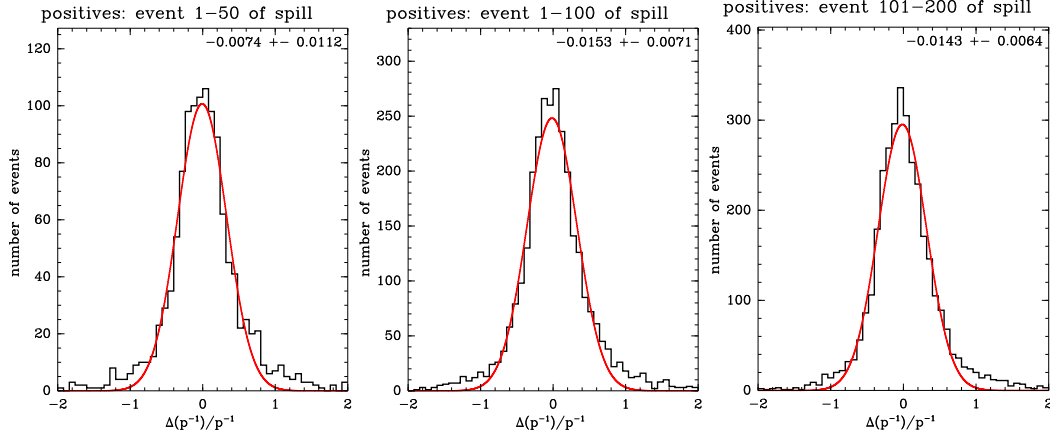
**Figure 6.** $\Delta(p^{-1})/p^{-1}$ plot for protons produced in $\pi^+$ p and pp elastic scattering, combining data from the 3, 5 and 8 GeV/$c$ primary beam momenta. Left panel: first 50 events in the spill, no corrections for dynamic distortions. Central panel: first 100 events in the spill, with corrections for dynamic distortions. Right panel: events 101–200 in the spill, with corrections for dynamic distortions.
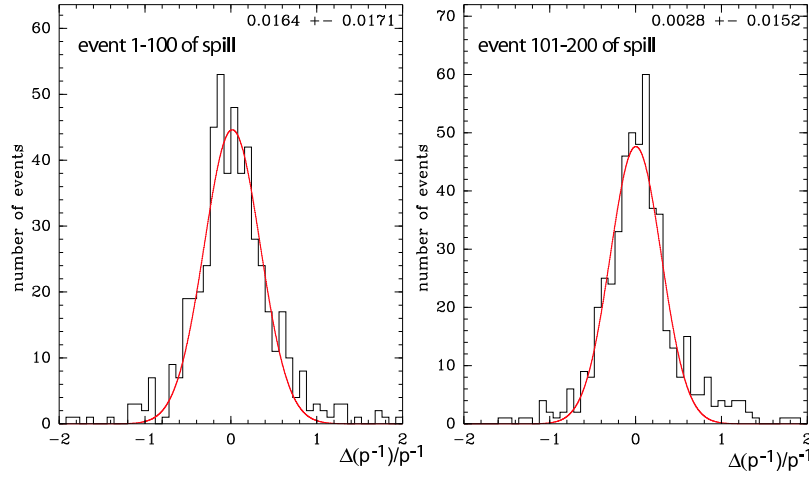


**Figure 7.** $\Delta p^{-1}/p^{-1}$ plot for $\pi^-$ p elastic scattering, combining data from the 3, 5 and 8 GeV/$c$ primary beam momenta, computed with the corrections for dynamic distortions of the TPC. Left panel: first 100 events in the spill, right panel: events 101–200 in the spill.

difference between the predicted and the measured $1/p$ (after corrections for the energy loss of the proton prior to entering the TPC), is shown in Fig. 6. As mentioned above, this procedure has an intrinsic 2% systematic error coming from the determination of the incoming beam momentum and from the angle measurement with the forward spectrometer.

The following results were obtained:

- The elastic scattering sample using the first 50 events (without corrections for dynamic distortions) and the elastic scattering sample using the events, corrected for dynamic distortions, from 1 to 100 and from 101 to 200 are fully compatible (see Fig. 6);

- With the larger statistics allowed by the use of 200 events per spill it is now possible to
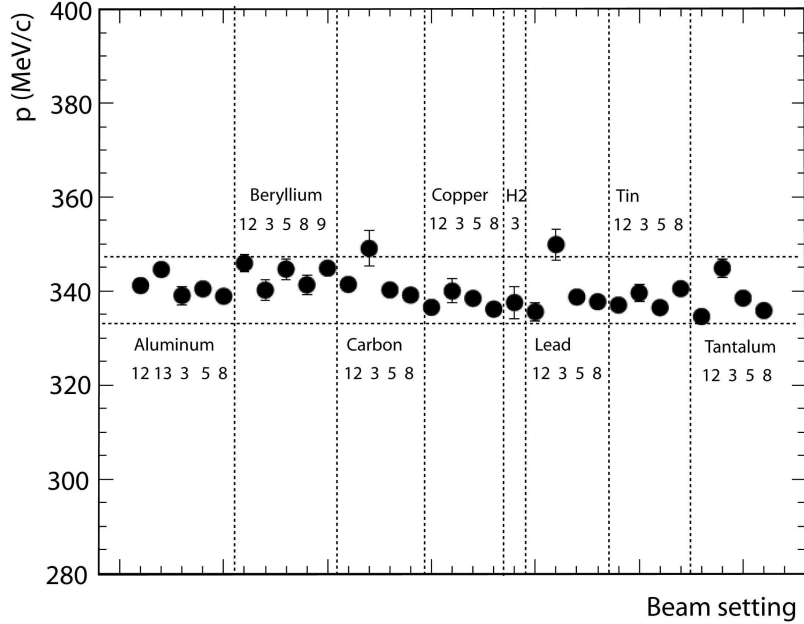
**Figure 8.** Average momentum of particles with a d$E$/d$x$ in the TPC corresponding to 7-8 MIP, as measured in 31 different settings. The horizontal dashed lines correspond to a variation of $\pm 2\%$ around the average value of 340 MeV/$c$. The different settings are labeled with the material of the target and the momentum, in GeV/$c$, of the incident beam.

compare "positives" ($\pi^+$ p and pp) (Fig. 6) and "negatives" ($\pi^-$ p) (Fig. 7).

The distribution for "positives" has an average $\Delta(p^{-1})/p^{-1}$ equal to $-0.0148 \pm 0.0047$ while the distribution for "negatives" has $\langle \Delta(p^{-1})/p^{-1} \rangle = 0.0096 \pm 0.0113$. The combination of the two polarities gives $\langle \Delta(p^{-1})/p^{-1} \rangle = -0.011 \pm 0.004$. Again, taking into account the systematic errors, we conclude that no bias on momentum is observed with a precision of 3%.

### 2.2.6 Stability of the elastic results with other settings

To check that the results obtained with the elastic events on the hydrogen target are stable in the other data taking settings, we have selected a narrow d$E$/d$x$ region corresponding to 7–8 MIP. In this region the pion contamination is negligible and protons have an average momentum of 340 MeV/$c$.

The average reconstructed momentum of protons in this band is shown in Fig. 8 for 31 different settings. All the settings provide an average momentum within $\pm 2\%$ around the average value of 340 MeV/$c$, demonstrating the stability of the momentum scale measured with elastics during the overall HARP data taking. Particles were only accepted when they were nearly perpendicular to the beam direction, so that the average $p_{\mathrm{T}}$ of this sample is 310 MeV/$c$.
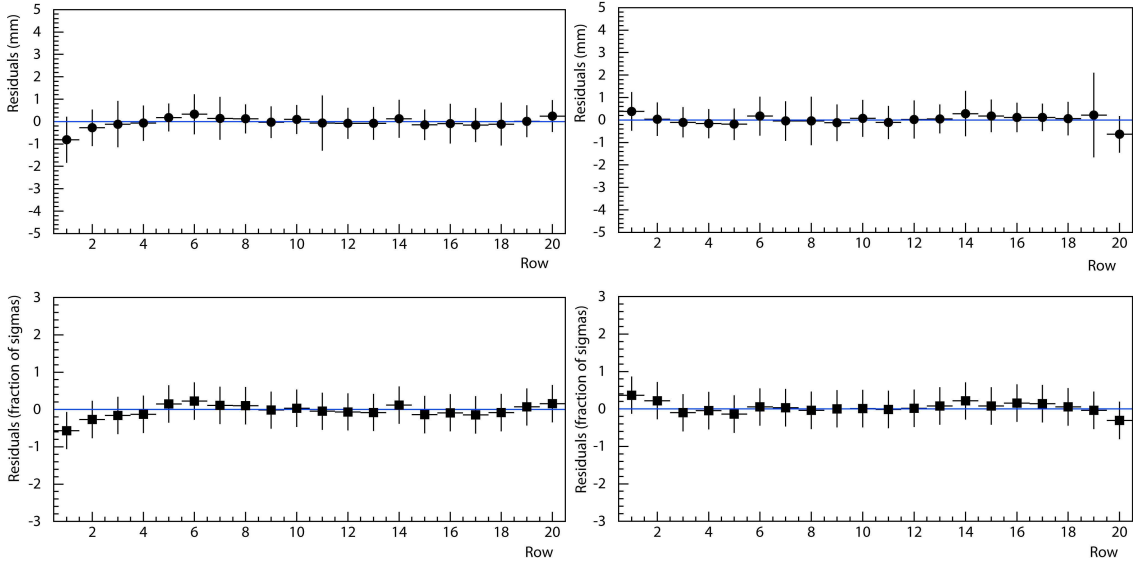
**Figure 9.** Left panel: the mean residual $\Delta(R\phi)$ for each pad row of the TPC measured using a $B$ field positive polarity setting (+5 GeV/$c$ Carbon target data). Top: $\Delta(R\phi)$ in mm. Bottom: $\Delta(R\phi)$ in fraction of RMS. Right panel: Same using a $B$ field negative polarity setting ($-5$ GeV/$c$ Carbon target data). Changing the $B$ field polarity, the swap in sign of the mean residuals in the innermost and outermost pad ring is clearly visible

## 3. Track residuals with positive and negative settings

A way to monitor the presence of residual distortions (when the dynamic distortion correction is not applied) is to look at the $\Delta(R\phi)$ difference between the coordinate of the track measured in each pad row of the TPC and the trajectory estimated by the circular fit. To do this we have selected tracks (vertex constrained) hitting the center of the RPC overlap to be able to fix an external point. The cuts applied in the standard analysis have been used. The same residual distributions can be obtained separately for positive and negative magnetic field direction. In this case an $E \times B$ effect changes sign for the two polarities. For this test we used a carbon 5% nuclear interaction length ($\lambda_I$) target with beam momenta of $\pm 5$ GeV/$c$ respectively.

The analysis of the distributions of the residuals shows that the biases are small (in the range of $\pm 200$ microns). As expected row number 1 (the innermost) and row number 20 (the outermost) display edge effects ($-800$ $\mu$m and $+300$ $\mu$m respectively) which are not fully addressed by the distortion correction for static misalignment between the inner and outer field cage voltages. The fact that the residual is larger in the inner row and of opposite sign to that in the outer row is consistent with the hypothesis that the effect is due to a residual electrostatic field, see Fig. 9 (left).

A further confirmation was obtained by looking at the residual distribution for the tracks of the $-5$ GeV/$c$ sample where the magnetic field polarity was inverted. In this last case the behaviour is the same but the sign of the residual of the innermost and outermost row is now inverted ($+380$ $\mu$m and $-635$ $\mu$m respectively), see Fig. 9 (right).

By excluding rows 1 and 20 from the fit, one can place a limit of less than 1% on the effect of the residual distortion effects on the momentum measurement.
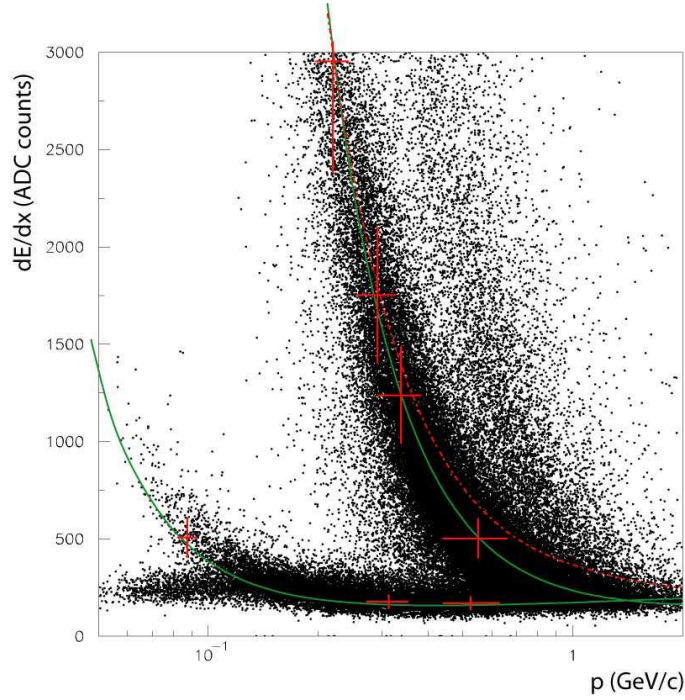
**Figure 10.** $dE/dx - p$ plot of HARP data, 5% Ta target at 5 GeV/$c$, fitted with the modified Bethe-Bloch function (see the text), including the resolution bars for every fitted slice in momentum and $dE/dx$. The bars are computed from the published momentum resolution and $dE/dx$ resolution for all points. The dashed curve is the $1/\beta^2$ curve.

## 4. Consistency checks of the momentum calibration with d$E$/d$x$

The d$E$/d$x$ cannot be used in HARP to estimate the momentum scale with a precision similar to the elastic scattering method because both the scale and offset calibration of d$E$/d$x$ are free parameters and the resolution in d$E$/d$x$, about 17%, is insufficient to achieve such a precision. Nevertheless, the d$E$/d$x$–$p$ plot provides a qualitative cross-check of the TPC momentum calibration. Indeed we find good agreement as shown in Fig. 10.

It has been claimed that the disagreement of the d$E$/d$x$ plots we published in [8] with a $1/\beta^2$ curve is a clear symptom of a TPC momentum bias, up to 15% [10]. Since the free parameters of the d$E$/d$x$ curve can only be fixed using the point at which particles are minimum ionizing, it will be immediately clear that a $1/\beta^2$ description, which reaches its minimum asymptotically, cannot be an adequate approximation as shown in the comparison of the correct curve and this simple approximation in Fig. 10. Since this was not immediately obvious to the authors of Ref. [10], we include here a rather pedantic discussion of d$E$/d$x$. The *average* energy loss is described with the standard Bethe-Bloch formula [11]:

$$-\frac{dE}{dx} = Kz^2\frac{Z}{A}\frac{1}{\beta^2}\left[\frac{1}{2}\ln\frac{2m_ec^2\beta^2\gamma^2T_{max}}{I^2} - \beta^2 - \frac{\delta(\beta\gamma)}{2}\right]. \tag{4.1}$$

For particle identification a truncated mean is tuned to correctly estimate the Landau peak position (discarding the 20% of points with the highest d$E$/d$x$), and not the mean d$E$/d$x$ (for
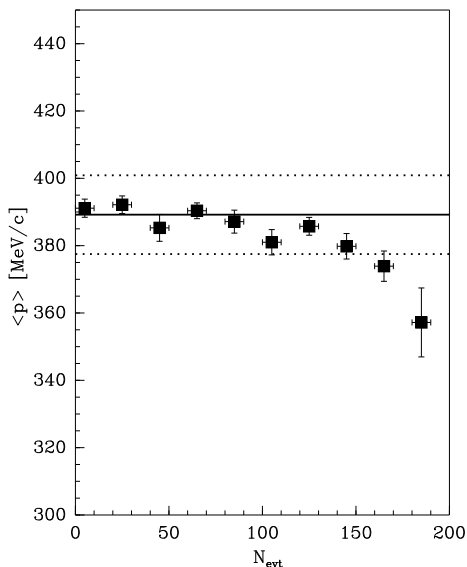
**Figure 11.** Average reconstructed momentum as a function of event number in spill for protons using a high value of d$E$/d$x$ for the selection. The analysis is performed for the combined data set taken with 3 GeV/$c$, 5 GeV/$c$, 8 GeV/$c$ and 12 GeV/$c$ beams on Be, C, Cu, Sn, Ta and Pb targets. The solid line shows the average for protons for the first 100 events in the spill. The two dotted lines show the ±3% variation around the average.

which the standard Bethe-Bloch theory applies). Hence each point on the d$E$/d$x$–$p$ scatter-plot represents the calculation of the most probable d$E$/d$x$ per TPC pad row, integrated over the tracks' effective path length across each pad row (therefore it represents the peak value of a convolution of Landau distributions). Its phenomenology can be described sufficiently accurately by a modified Bethe-Bloch formula [12], as shown in Fig. 10: the d$E$/d$x$ for protons, pions, the positions of the d$E$/d$x$ of a minimum ionizing particle (MIP), and intersection points of the bands for different particle types are all consistent.

To avoid the effect of dynamic distortions the above analyses were done using only the first 50 events in each spill. It was checked that the constrained fit remains stable, well within 3%, for about 100 events in the spill as will be described in the following section.

### 4.1 Stability against dynamic distortions

One can select samples of tracks with a well defined momentum by accepting narrow enough d$E$/d$x$ intervals in the region of high values (the so-called "1/$\beta^2$" region). The d$E$/d$x$ resolution is sufficient to select such a proton sample with only a 10% RMS spread in "true" momentum. If the measured average momentum of such samples is compared as a function of event number in the spill $N_{evt}$ strong constraints on the influence of dynamic distortions on the momentum measurements can be obtained.

In this analysis particles were selected in narrow bands of d$E$/d$x$ in regions where d$E$/d$x$ depends strongly on momentum. To select a sample with the highest possible momentum, the protons were further required to reach the RPC system (low momentum protons would be absorbed before reaching the RPCs). A further selection 1.0 rad < $\theta$ < 1.5 rad ensures a limited range of

$p_T$. In addition to a momentum selection also a PID-selection is performed with the same cuts. The analysis was performed for the combined data set taken with 3 GeV/$c$, 5 GeV/$c$, 8 GeV/$c$ and 12 GeV/$c$ beams on Be, C, Cu, Sn, Ta and Pb targets.

The average momentum obtained from a Gaussian fit to the momentum distribution shows that the average momentum stays constant within a few percent up to $N_{\text{evt}} = 100$ at $p_T \approx 350$ MeV/$c$ (see Fig. 11).

One observes that the behaviour is not compatible with a linear dependence as a function of time but the average momentum stays constant over a long period before a downward trend sets in. One of the reasons is the fact that the distortion effect does not have a linear dependence at the beginning of the spill, owing to the fact that the first ions need to exit the amplification zone before they distort the field in the drift zone. This is shown in a little more detail in the Appendix. This effect "protects" the first fifty events in the spill very efficiently. Another reason for increased stability of the constrained fit under the condition of distortions is simply that the weight of the vertex constraint compensates very well for the distortions, up to the point where, when dynamic corrections are not applied, the tracks are so distorted that the reconstruction efficiency is affected.

It has been shown with elastic scattering that the absolute track finding efficiency does not change as a function of event number in the spill. This result indicates that the distortions are continuous and smooth as a function of $z$ and $R$. However, once quality criteria are applied, mainly the requirement that the tracks emerge from the target, the efficiency is reduced when the distortions are increasing during the growth of the ion charge. Since this requirement removes tracks shifting out of the acceptance at one side, and since the measurements of curvature and of the minimum distance to the interaction point are correlated, the deviation of the average measured momentum from a constant is thus a single-sided efficiency effect.

The $p_T$-range covered by this cross-check represents a large range of the kinematic domain used in the analysis.

## 4.2 Sagitta errors from momentum-angle correlations

Using a sample of tracks within a fixed interval of d$E$/d$x$ where the average momentum is $\sim$ 340 MeV/$c$, and considering that $p_T = p_{\text{tot}} \sin\theta$, it is possible to look for a sagitta bias (acting on $p_T$) through any correlation between $\langle p \rangle$ and $\sin\theta$. Unlike previous analyses where the RPC hits were used to set a minimum range, here such a requirement was avoided not to introduce an angular dependence in the definition of the average energy of the sample. From the fits to Fig. 12 (left) we conclude that a null bias is measured with a precision of about 3%. This analysis has been repeated using positive and negative pions and the correction for dynamic distortions with incoming $\pi^+$ in the positive beam and $\pi^-$ in the negative beam (Ta target, 8 GeV/$c$). As shown in Fig. 12 (right), for both magnet polarities there is no significant dependence on $\sin\theta$.

Since the curvature of the protons and of distortions (if of the $E \times B$ type) are both inverted, the slope for protons (if any) is expected to have the same sign for positive and negative beams. The fact that there is no significant dependence on $\sin\theta$ confirms the reliability of the HARP TPC calibration.
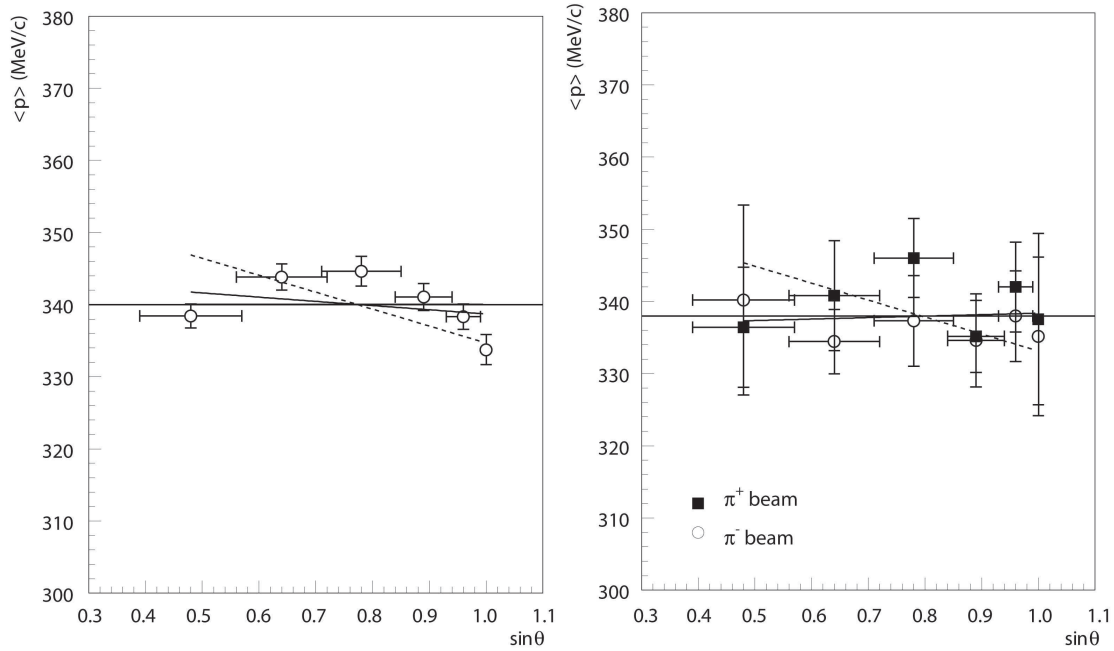
**Figure 12.** Left panel: average momentum in a fixed slice of d$E$/d$x$ as a function of $\sin\theta$. Data are collected with Be, C, Cu, Sn, Ta and Pb targets at 3, 5 and 8 GeV/$c$, no correction for dynamic distortions. A fixed shift in sagitta would show up as a linear change of average momentum. These data have been fitted with a constant term, with a linear function (the best fit corresponds to a momentum bias of $\sim 2.5\%$ at 500 MeV/$c$) and with a linear function with a slope corresponding to a 10% bias (dashed line). While the constant term is compatible with the linear function ($\Delta\chi^2 = 0.8$), a 10% bias has $\Delta\chi^2 \simeq 20$. Thus, it is excluded at more than 5 sigma level. Right panel: same analysis for $\pi^+$ (black squares) and $\pi^-$ (open circles) incident beams and with the full spill correction for dynamic distortions. These data were taken with opposite magnetic field polarities. Data are collected for 8 GeV/$c$ incident beam on Ta target only. A fixed shift in sagitta would show up with the same slope for positives and negatives. In this case, given a smaller statistics, a 10% bias is excluded at about 90% C.L. ($\Delta\chi^2 \simeq 4.1$).

## 5. Comparison with time-of-flight measurements

The HARP RPC system [13] is positioned as a barrel around the TPC chamber, about 50 cm from the interaction target. It can in principle be used to check the momentum calibration comparing the $\beta$–$p$ relation of pions and protons, where $\beta$ is measured using the time-of-flight to reach the RPC system.

This cross-check is limited in precision due to the short flight distance of the particles and the rather large corrections needed to convert the measured threshold crossing time into a measurement of time-of-arrival of the particle. For example the range of the correction for the "time-slewing" of the threshold crossing time for different measured integrated charge collected in the RPCs is 2 ns, similar to the total time-of-flight of pions to reach the RPCs [13]. As an additional complication, the momentum range of the particles for which a $p$–$\beta$ comparison can be made is in the region where pions are minimum ionizing and where protons are heavily ionizing (with a different d$E$/d$x$ by a factor of up to 8). Thus one first has to ascertain that the response of the RPC system is well understood before one can use the time-of-flight as a mean to calibrate the momentum measurement
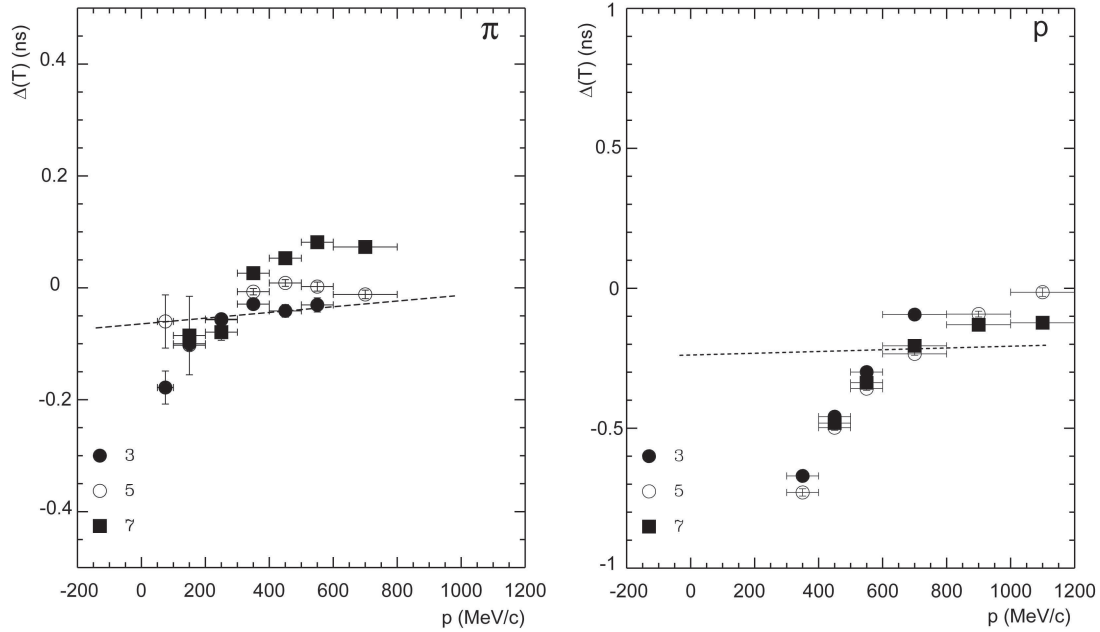
**Figure 13.** Analysis of Δ TOF = (measured − predicted) time-of-flight for pions (left panel) and protons (right panel). The measured time is provided by the RPC signal time and the predicted time is based on the track momentum measured in the TPC. The numbers refer to RPC pad ring (equivalent to $Z$ position; with pad 3 in the most backward direction). Whereas the pion data are centered near zero, the proton data are shifted to negative times with a positive slope. The dashed line is the prediction for Δ TOF for a sagitta bias of 1 mm and a track length of 0.5 m.

in the TPC.

Fig. 13 taken from reference [13] shows the difference of the time-of-arrival measured with the RPCs, $t_{\mathrm{m}}$, and the time-of-arrival predicted using the momentum measured in the TPC, $t_{\mathrm{p}}$.

This plot had been used in [10] to claim a 15% bias in the HARP TPC momentum scale.

If a momentum bias would be caused by an error in the measurement of the trajectory sagitta, it would reflect on the $\beta$ of protons and not on the $\beta$ of pions, which already saturate $\beta$ at the HARP momenta. The RPC calibration has been performed using pions, so that one would expect that these display a vanishing average offset as is the case in Fig. 13. However, the behaviour of the measured $\Delta(TOF)$ for protons does not agree with that predicted by the sagitta model, see Eq (1.1). While data, Fig. 13, exhibits a clear slope, the sagitta model predicts a rather flat dependence of $\Delta(TOF)$ on the measured momentum. This flatness comes from the particular momentum range of the protons where $\delta(p)/p$ increases linearly with $p$, while $\Delta(TOF)$ decreases with $p$ because $\beta$ of the protons saturates.

The question whether the RPC time measurement suffers from systematic effects due to the large difference in primary ionization caused by pions and protons in the momentum range available for these calibrations had been addressed with a dedicated RPC calibration analysis studying proton and pion elastic scattering off the cryogenic hydrogen target and reported in reference [14].

As for the measurement of the momentum scale, see Section 2, such a measurement makes it possible to send a "controlled beam" of slow protons through the TPC and towards the RPC system
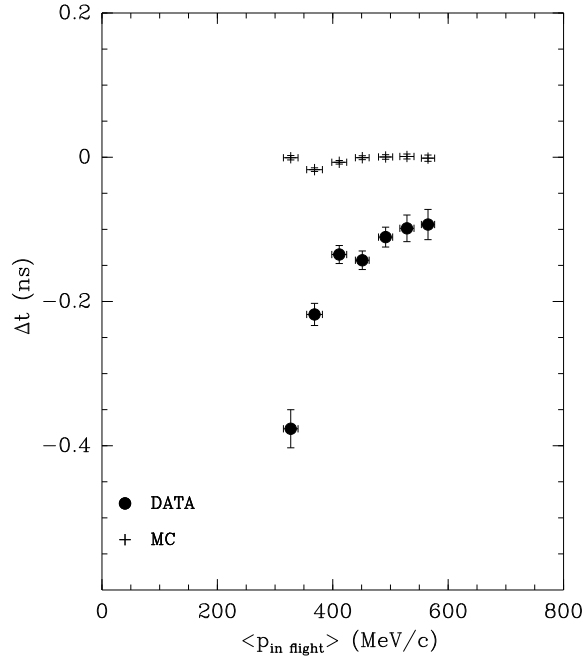
**Figure 14.** The difference of the time offset measured in pad ring 3 from the expected time offset for protons as a function of the momentum along its flight path (in the gas volume of the TPC). The filled circles show the results of measurements using elastic scattering on hydrogen, the points without marker represent the simulation of the measurement using the same reconstruction procedure. The momentum was predicted using the kinematics of elastic scattering. Consistency of the simulated time difference with zero shows that the prediction of the flight time (and thus of the momenta) using the elastic scattering kinematics and Monte Carlo corrections in the reconstruction procedure for respective energy losses are correct. From reference [14].

without the need to measure the momentum of the recoil proton with the TPC.

An exposure of the HARP detector where a 5 GeV/$c$ beam of protons and pions is directed onto a 60 mm long liquid hydrogen target was used.

Results of this analysis are shown in Fig. 14. Due to the kinematics of elastic scattering the vast majority of selected recoil protons which reach the RPC system is measured in pad ring 3.

The data exhibit a clear deviation pointing to a difference in RPC time response to protons as a function of the momentum. The difference can only be due to the different response of the RPCs to heavily ionizing compared to minimum ionizing particles. The observed effect accounts for the largest fraction of the absolute values and the shape of the deviations observed in Fig. 13.

The remaining difference observed between the points of Fig. 13 and Fig. 14 is of the order of $(150 \pm 100)$ ps at 450 MeV/$c$, where the error is estimated from the spread of the points for the different pad rings. The central value of 150 ps corresponds to a momentum shift of $\approx$4.5% at 450 MeV/$c$.

Several important systematic errors affect this measurement:

- The momentum prediction with elastic scattering needs a correction for energy loss in the region of the inner field cage of the TPC. Although the description of the physical processes is very accurate it is possible that a slightly larger amount of material is present than that

accounted for in the calculations (the opposite is excluded). If the calculation is repeated with 10% more material a 1%–2% shift in predicted momentum is induced which would *reduce* the apparent difference.

- Background hits in the RPC pads can only create an earlier time measurement, since single-hit TDCs were used to read out the system. Given the charged track multiplicities and the corresponding number of converted photons from $\pi^0$ decays this overlap probability is estimated to be $\approx 5\%$. The effect of such background is not easy to estimate, but the resulting measurement is shifted towards shorter time-of-arrival. This background is not present in elastic scattering events.

- There is a 20 ps–30 ps difference in measured arrival time for $\sim 400\,\mathrm{MeV}/c\ \pi^+$ versus $\pi^-$. However in the negative beams this is as small as 0 ps–10 ps. The difference with opposite B field shows already that the RPCs have this kind of systematic. The latter can be due to the position-dependent slewing correction to the amplifier position which has as maximum swing 180 ps, and assumes exact knowledge of where the first electron was detected. (there is a symmetry breaking due to the amplifier position always to one side.)

- There is a 1% difference in the average pulse-height for $\pi^+$ and $\pi^-$ with $\sim 400\,\mathrm{MeV}/c$ in the 90° direction. There the production cross-sections are equal. The difference can come from the $E \times B$ effect for the avalanche electrons which can induce a different space-charge effect due to the different angle of incidence of the $\pi^+$ and $\pi^-$ in the RPC measurement gap due to the opposite curvature of their trajectories in the TPC. This can explain a $\pm 15$ ps difference of threshold crossing, keeping in mind that the threshold was relatively high, considering that the full time slewing correction is $\sim 2000$ ps.

Therefore, the RPC system cannot provide a cross-check of the same quality as the elastic scattering data. As a conclusion, the observed time-of-arrival of protons at the RPC barrel is consistent with an unbiased measurement of momentum within a relatively large error of 5%.

## 6. Conclusions

Asserting the correctness of the momentum reconstruction in the HARP TPC has not been easy, as can be expected from a chamber affected by a large number of dead channels, cross-talk, static and dynamic distortions in the absence of the possibility to use a direct particle beam for calibration. By a series of dedicated cross-checks with benchmarks, the experimental verification could nevertheless be made. This allowed us to conclude that the TPC momentum reconstruction developed by the HARP collaboration is correct within the precision of $\pm 3\%$. This confirms the systematic error associated to the momentum scale used in determining the large angle production of charged pions by protons in [8, 9].

The calibrations and cross-checks include

- reconstruction of the missing mass squared of pp elastic scattering data;

- comparison of the momentum of the proton scattered at large angle as measured by the TPC and as calculated from the scattering angle of the forward particle in pp and $\pi^{\pm}$p elastic scattering events;

- dependence of residuals upon polar angle and upon magnetic field polarity reversal, for tracks reconstructed with and without vertex constraint during the fit;

- absence of slope in the momentum versus $\sin\theta$ plots in a fixed slice of $dE/dx$;

- comparison of the $dE/dx$ curves in the region of high ionization where the ionization varies very quickly with momentum, allowing a sensitive verification of the momentum scale.

We also revisited methods of lesser precision, such as $dE/dx$ in the region near the minimum ionization, for which we found that it is crucial to use a complete Bethe-Bloch formula to reach reasonable conclusions. Once this is done we find a good match between $dE/dx$ theoretical curves and our data, in comfort of our momentum reconstruction.

Finally a careful analysis of the time response of the RPC system ascertains that no momentum bias is present beyond the uncertainties of this method. While investigating any possibility of systematic effect on the momentum measurement, the presence of a systematic effect in the time measurement of the RPCs has been demonstrated.

As a conclusion, none of the benchmarks has revealed any significant bias in the momentum measurement beyond a systematic error of 3% for the momentum scale in the TPC.

**Figure 15.** Average $d'_0$ as a function of event number in spill for 8.9 GeV/$c$ Be data. (left panel uncorrected; right panel: dynamic distortion corrections applied.) After the "default" correction for the static distortions (equal for each setting) a small residual effect at the beginning of the spill is visible at $N_{evt} = 0$ (left panel). This is due to the fact that the inner and outer field cages were powered with individual HV supplies. A setting-by-setting correction compatible with the reproducibility of the power supplies is applied for the data of the right panel together with the dynamic distortion correction.

## A. Appendix: Treatment of the Dynamic Distortions

Given the beam intensity, the data acquisition rate and the target length (5% of the nuclear interaction length), it is computed that HARP operated dead time larger than 90%. The electrons are normally amplified near the TPC pad plane with an amplification factor of the order of $10^5$, producing an equivalent number of Argon ions. Any inefficiency of the gating grid at the level of $10^{-3}$ or even $10^{-4}$ would let an overwhelming number of ions drift into the TPC gas volume.

This indeed turns out to be the case. The dynamic distortions can be monitored using the average value of the extrapolated minimum distance of secondary tracks from the incoming beam
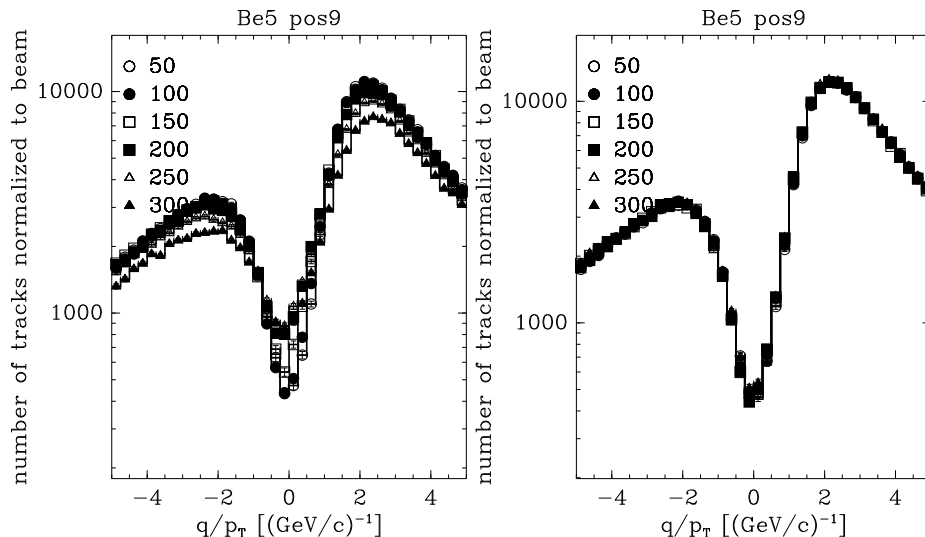
**Figure 16.** Analysis of $Q/p_T$ for the highest statistics data sample: p-Be at 8.9 GeV/$c$. Left panel: distortions are not corrected; six curves are drawn, each for the next 50 events in the spill. Right panel: dynamical distortions are corrected; the six curves are almost not distinguishable

particle trajectory $d'_0$. This is a similar procedure as the one being used for the STAR TPC [15]. Using calibration data sets, the deterioration of the performance of the detector, see Fig. 15 (left), is determined as a function of the strength of the distortions characterized by an average value of $d'_0$: for each particular setting only that part of the data for which the systematic error was under control was used for the first analysis (of the order of 30% of available statistics) [8, 9]. As a second step, a physics model fully describing the time development of dynamic distortions during physics spills has been developed and benchmarked, as well as a correction algorithm [16] implemented.

In addition to the physics model, direct measurements of the displacements of the positions measured at the pad plane of the TPC were performed by predicting the full track trajectory in space using elastic scattering kinematics. The direct measurement and the model show good agreement, indicating that the effect is fully understood. The effects of this correction can be appreciated in Fig. 15 (right). The comparison of results obtained using the uncorrected first part of the spill, as in the first HARP analysis, with those using the full corrected spill (see Fig. 16) shows excellent agreement. This provides an *a posteriori* confirmation with 2 to 3 times better statistics that the approach used in the first HARP analysis was correct. This is not unexpected, since, owing to their limited mobility the first ions created in the amplification region need about 25 ms to reach the drift region and subsequently the steady flow of ions into this region only starts approximately 100 ms after the start of the spill, with a gradual transition between these two regimes.

## References

[1] M.G. Catanesi *et al.* [HARP Collaboration], *Proposal to study hadron production for the neutrino factory and for the atmospheric neutrino flux*, CERN-SPSC/99-35 (1999).

[2] M. G. Catanesi *et al.* [HARP Collaboration], *The HARP Detector at the CERN PS*, Nucl. Instrum. Methods **A571** (2007) 527.

[3] M. G. Catanesi *et al.* [HARP Collaboration], *" Measurement of the production cross-sections of $\pi^{\pm}$ in p-C and $\pi^{\pm}$-C interactions at 12 GeV/c", Astropart. Phys.* **29** (2008) 257. arXiv:0802.0657 [astro-ph].

[4] M. G. Catanesi *et al.* [HARP Collaboration], *Measurement of the production cross-section of positive pions in p Al collisions at 12.9 GeV/c* , Nucl. Phys. B **732** (2006) 1, [arXiv:hep-ex/0510039].

[5] M. G. Catanesi *et al.* [HARP Collaboration], *Measurement of the production cross-section of positive pions in the collision of 8.9 GeV/c protons on beryllium*, Eur. Phys. J. C **52** (2007) 29, [arXiv:hep-ex/0702024].

[6] M. Anfreville *et al.*, *The drift chambers of the Nomad experiment*, Nucl. Instrum. Methods **A481** (2002) 339.

[7] M. Baldo-Ceolin *et al.*, *The time-of-flight TOFW detector of the HARP experiment: construction and performance*, Nucl. Instrum. Methods **A532** (2004) 548.

[8] M. G. Catanesi *et al.* [HARP Collaboration], *Measurement of the production of charged pions by protons on a tantalum target*, Eur. Phys. J. C **51** (2007) 787, [arXiv:0706.1600].

[9] M. G. Catanesi *et al.*, [HARP Collaboration], *Large-angle production of charged pions by 3 GeV/c–12 GeV/c protons on carbon, copper and tin targets*, Eur. Phys. J. C **53** (2008) 177 [arXiv:0709.3464 [hep-ex]]. M. G. Catanesi *et al.*, [HARP Collaboration], *Large-angle production of charged pions by 3 GeV/c–12.9 GeV/c protons on beryllium, aluminium and lead targets*, Eur. Phys. J. C **54** (2008) 37 [arXiv:0709.3458 [hep-ex]].

[10] V. Ammosov *et al.*, *Comments On: The HARP Detector At The Cern Ps,* Nucl. Instrum. Meth. A **571** (2007) 562. V. Ammosov *et al.* , *Comments on TPC and RPC calibrations reported by the HARP Collaboration,* JINST **3** (2008) P01002 [arXiv:0711.2216 [hep-ex]].

[11] Particle Data Book 2006, page 258.

[12] V.M. Grishin, G.I Merson, *A simple method for realistic estimation of the most probable energy loss in thin gas layers*, Nucl. Instrum. Methods **A274** (1989) 551.

[13] M. Bogomilov *et al.*, *Physics Performance of the Barrel RPC System of the HARP Experiment*, IEEE Transactions On Nuclear Science, Vol. 54, No. 2, April 2007, pp.342-353.

[14] A. Artamonov *et al.*, *The Time Response of Glass Resistive Plate Chambers to Heavily Ionizing Particles*, 2007 *JINST* **2** P10004, [arXiv:0709.3756 [physics.ins-det]].

[15] G. Van Buren *et al.*, *Correcting for distortions due to ionization in the STAR TPC*, Nucl. Instrum. Methods **A566** (2006) 22.

[16] A. Bagulia *et al.*, *On the HARP TPC dynamic distortions*, paper in preparation.